*Article*

# Green Synthesis of Silver Nanoparticles with Extract of Indian Ginseng and In Vitro Inhibitory Activity against Infectious Bursal Disease Virus †

Bhaskar Ganguly [1],*, Ashwini Kumar Verma [2], Balwinder Singh [3], Arup Kumar Das [2], Sunil Kumar Rastogi [1], Alireza Seidavi [4], Diamanto Lazari [5] and Ilias Giannenas [6],*

[1]  Animal Biotechnology Center, Department of Veterinary Physiology and Biochemistry, College of Veterinary & Animal Sciences, G. B. Pant University of Agriculture & Technology, Pantnagar 263145, India

[2]  Department of Surgery and Radiology, College of Veterinary & Animal Sciences, G. B. Pant University of Agriculture & Technology, Pantnagar 263145, India

[3]  Electron Microscopy Laboratory, Department of Veterinary Anatomy, College of Veterinary & Animal Sciences, G. B. Pant University of Agriculture & Technology, Pantnagar 263145, India

[4]  Department of Animal Science, Rasht Branch, Islamic Azad University, Rasht 41335-3516, Iran

[5]  Department of Pharmacognosy-Pharmacology, School of Pharmacy, Aristotle University, 54124 Thessaloniki, Greece

[6]  Laboratory of Nutrition, School of Veterinary Medicine, Aristotle University, 54124 Thessaloniki, Greece

*   Correspondence: vetbhaskar@gmail.com (B.G.); igiannenas@vet.auth.gr (I.G.); Tel.: +91-9411159689 (B.G.); +30-2310999937 (I.G.); Fax: +91-5944-233473 (B.G.)

†   This work was part of PhD research of the first author.

**Abstract:** Infectious bursal disease virus (IBDV) is a serious poultry pathogen responsible for causing major economic losses to the poultry industry globally. The virus is closely related to several other important viral pathogens of fishes, crabs, and mollusks and evolutionarily related to important viral pathogens of humans. Previously, we demonstrated the inhibition of this virus by the extracts of roots of *Withania somnifera* Dunal, commonly known as Indian ginseng, both in vitro and in vivo. Furthermore, many studies reported the inhibition of diverse types of viruses by nanoparticles of silver. In the present study, we investigated the inhibitory effect of silver nanoparticles obtained by green synthesized with Indian ginseng extract against IBDV. Conditions for the synthesis of silver nanoparticles were optimized, and the nanoparticles thus obtained (WS AgNPs) were characterized physically. Thereafter, the maximum non-cytotoxic dose of these nanoparticles for treating chicken embryo fibroblasts (CEF) was determined. Treatment of IBDV-infected CEF with the WS AgNPs decreased the infective virus titer by >93%, intracellular viral load by >71%, and virus-induced cytopathy by >51%, demonstrating the strong inhibitory effect of the WS AgNPs against IBDV, and encouraging similar applications against related veterinary and human viruses.

**Keywords:** infectious bursal disease; virus; nanoparticle; silver; Indian ginseng; *Withania somnifera*

## 1. Introduction

Infectious bursal disease (IBD) is an acute, highly contagious, and immunosuppressive viral disease of chickens resulting in severe economic losses [1]. The causative virus (IBDV) is a member of the genus *Avibirnavirus* of the *Birnaviridae* family, represented by non-enveloped viruses bearing a bipartite, double-stranded RNA genome. Classical IBDV strains cause 10–50% mortality, whereas hypervirulent strains, causing 50–100% mortality, incur much higher losses [2]. IBD remains enzootic in most parts of the world despite the resolution for its global control passed in the year 1995 by the World Organization for Animal Health [3]. Satisfactory therapeutic interventions are unavailable, and the determination of the appropriate age for vaccination is a challenge [1]; immunization with

inactivated or low-virulence virus affords insufficient immunity and vaccination with a virulent virus itself causes immunosuppression [4]. The virions are very hardy [1], and facility disinfection is difficult to achieve after outbreaks. Thus, the need for novel agents for the control of the disease becomes imperative.

Metallic nanoparticles, notably those of silver, have been reported to possess good antiviral activity [5], and chemically synthesized silver nanoparticles inhibit IBDV in ovo [6]. Silver nanoparticles exhibit promising cytoprotective activities towards human immunodeficiency virus (HIV)-infected T cells [7]. Silver nanoparticles have also been shown to be capable of inhibiting several viruses such as hepatitis B virus [8], monkeypox virus [9], human simplex virus-1 [10], adenovirus type 3 [11], human parainfluenza virus type 3 [12], H1N1 influenza virus [13], vaccinia virus [14], H3N2 influenza virus [15], peste des petits ruminants virus [16], and chikungunya virus [17] in vitro.

Unlike physical methods that tend to be technology- and cost-intensive, and chemical methods that use noxious chemical agents, the green synthesis of metallic nanoparticles is a much simpler approach, which utilizes the reducing activity of plant extracts for the conversion of inorganic salts to metallic particles. Some organic components, such as polysaccharides or glycoproteins, present in the extract further stabilize the nanoparticles against aggregation [5]. The green synthesis of metallic nanoparticles has been reported using a very diverse range of plant extracts and phytoactives [5], which also includes extracts of leaves of *Withania somnifera* Dunal (WS) [18,19]. *Withania somnifera* is recognized as a wild plant in northwest India [20]. More than 39 active compounds have been identified after extensive chemical composition research. Recently, many phytochemical components have been identified, including total phenol, 12 alkaloids, 40 withanolides, and numerous sitoindosides [21]. In plants of the *Solanaceae* family, a very potent antioxidant molecule has been shown to increase three naturally occurring antioxidant enzymes, according to several studies [22]. Commonly known as Indian ginseng, the roots of WS possess very strong reducing activity [23] and should likely facilitate the green synthesis of silver nanoparticles. Moreover, Indian ginseng has been shown to exert good inhibitory activity against IBDV both in vitro [24,25] and in vivo [26]. The current study aimed to test the in vitro inhibitory activity of silver nanoparticles green-synthesized with an extract of Indian ginseng against IBDV.

## 2. Materials and Methods

### 2.1. Extract, Cells and Virus

Identical extracts of WS roots, primary chicken embryo fibroblast (CEF) culture, and infectious bursal disease virus, described previously [25], were used in the present study.

### 2.2. Nanosynthesis and Yield Optimization

Briefly, 10 mL of methanol:chloroform:water (12:5:3, v/v) (MCW extract) (10 µg/mL) of WS roots were added to 100 mL of 10 mM solution of silver nitrate. The solution was placed in a microwave (80 MHz) oven for 30 s and allowed to stand overnight in the dark. The visible appearance of a characteristic cola-colored suspension was considered the first indication of the successful synthesis of silver nanoparticles (WS AgNPs); the reaction conditions for nanosynthesis were further optimized for better quality and quantity of WS AgNPs. A two-step approach was used to determine the optimum conditions of nanosynthesis; first, the concentration of the extract was varied (5, 7.5, 10, 12.5, and 15 µg/mL), maintaining a constant volume (10 mL). Thereafter, the volume of the extract was varied (5, 8, 10, 12, and 15 mL), maintaining a constant concentration (12.5 µg/mL). The WS AgNPs synthesized during each reaction were characterized by UV-Vis spectrophotometry to determine the reaction conditions for optimum yield, according to Ganguly et al. [23].

### 2.3. Characterization of Nanoparticles

The WS AgNPs were preliminarily characterized by UV-Vis spectrophotometry. The absorbance of the suspension of WS AgNPs was recorded against distilled water over a

wavelength range of 250–700 nm at a resolution of 1 nm. WS AgNPs were precipitated from the suspension through repeated centrifugation (16,000 rpm) until the supernatant turned visibly clear. Excess moisture was blotted off the precipitated nanoparticles, which were weighed thereafter to derive the yield.

For further characterization, Fourier transform infrared (FTIR) spectra of nanoparticles were recorded in transmittance mode from 4000 to 400 cm$^{-1}$ on a Thermo Nicolet 6700 FT-IR spectrometer at a resolution of 4 cm$^{-1}$ and the spectra, representing the average of 32 scans, were plotted. Thereafter, X-ray diffraction (XRD) scans were acquired on a Rigaku D/Max-2200 diffractometer at room temperature using monochromatic Cu-K$\alpha$ radiation ($\lambda$ = 0.154 nm) operated at 40 kV and 30 mA at a 2$\theta$ angle pattern. Finally, the suspension of nanoparticles was bath-sonicated for 30 min and filtered through a 0.22 $\mu$ filter. A small droplet of the filtrate was placed on a copper grid, and the excess was blotted off. After drying, the grid was observed in a Jeol JEM 1011 transmission electron microscope; the size–distribution of the nanoparticles was derived based on the sizes of 200 nanoparticles measured using the in-built software.

## 2.4. In Vitro Cytotoxicity

The maximum non-cytotoxic dose of WS AgNPs for treating CEF was determined using five different methods. An alamarBlue assay was performed using a commercial alamarBlue cytotoxicity assay kit (HiMedia Labs, India) as per the manufacturer's recommendations. A diphenylamine (DPA) assay was performed as described by Chang et al. [27], and a combined crystal violet (CV), MTT assay, and neutral red (NR) assay were performed as described by Pretorius et al. [28]. The cytotoxicity assays were performed in triplicate.

## 2.5. Viral Inhibition Assays

Virus titration was performed as per Kibenge et al. [29], and the titer was expressed as median tissue culture infective doses (TCID$_{50}$) per mL of the culture supernatant. In total, 100 $\mu$L of log$_{10}$ dilutions of the culture supernatant, obtained 48 h post-infection (hpi) by repeated freeze–thaw, were prepared in EMEM and added to 80–90% confluent CEF monolayers grown in 96-well cell culture plates. The TCID$_{50}$ of the virus was determined by the modified Spearman–Kaerber method [30]. Next, a microtiter plate viral inhibition assay was used to determine the reduction in TCID$_{50}$ of the virus in the presence of the nanoparticles. A 'constant inhibitor—decreasing virus' approach was used; 96-well plates with 80–90% confluent CEF monolayers were taken, and the spent growth medium was replaced with fresh maintenance medium along with the virus and nanoparticle suspension. The inhibition of the virus was expressed as a percentage decrease in the virus titer at 48 hpi in the presence of the nanoparticles.

RT-PCR was also performed for the comparison of viral loads in IBDV-infected CEF treated with either WS AgNPs, MCW extract, or silver nitrate for 48 h. Total RNA was extracted from the CEF at 48 hpi using a HiPurA Total RNA miniprep kit (HiMedia Labs, India) according to the manufacturer's recommendations. RT-PCR was performed using a HiScript One-Step RT-PCR Kit (HiMedia Labs, India), and semi-quantification of viral load was performed in terms of relative expression of *vp2* based on integrated densitometric values (IDV) determined by Image J *v.*1.48 as described previously [26].

Lastly, virion stability studies were performed. The viral suspension was incubated with WS AgNPs for 0, 3, or 6 h. Nanoparticles were separated by centrifuging at 16,000$\times$ *g* rpm for 10 min, and the treated virus was used to infect CEF cells. The plate was allowed to incubate, and an MTT assay was performed at 48 hpi. Mock infection or mock treatment with fresh culture medium served as a control in the respective assays. All virological assays were performed in triplicate.

*2.6. Statistical Analyses*

All statistical operations were performed using Daniel's XL Toolbox *v*.6.53. Statistical comparison between different groups was determined based on analysis of variance (ANOVA) followed by Tukey's multiple comparisons as a post hoc test.

## 3. Results and Discussion

The visible color change in silver nitrate solution, indicative of successful nanonization, is shown in Figure 1. Figure 1c shows the color of the nanoparticle suspension obtained upon the optimization of reaction conditions. UV-Vis spectrophotometry was performed to confirm the formation of nanoparticles. AgNPs, upon UV-Vis spectrophotometry, are known to exhibit a surface plasmon resonance (SPR) peak in the wavelength range of approximately 400–450 nm; a single, sharp peak represents monodisperse nanoparticles of uniform size [31]. Optimum nanosynthesis, which can be influenced by several factors [23], was achieved when 12 mL of MCW extract (12.5 µg/mL; *w/v* in water) was used per 100 mL of 10 mM silver nitrate (Figure 2). The yield of freshly precipitated WS AgNPs was approximately 81.3 mg/mL on a wet weight basis. Previously, Marslin et al. [19] obtained silver nanoparticles with an aqueous extract of WS leaves but not its roots. In addition to the factors such as the geographical source, altitude, climatic conditions [32], and the stage of harvesting that influence the composition of the plant parts, a significant difference in the reducing activities of aqueous and MCW extracts [23] may also be responsible for such results. Roots are the most commonly used plant part of WS in indigenous medicinal practices [26] and successful nanonization with root extracts has encouraging commercial implications.



|     |     |     |
| --- | --- | --- |
| (**a**) | (**b**) | (**c**) |
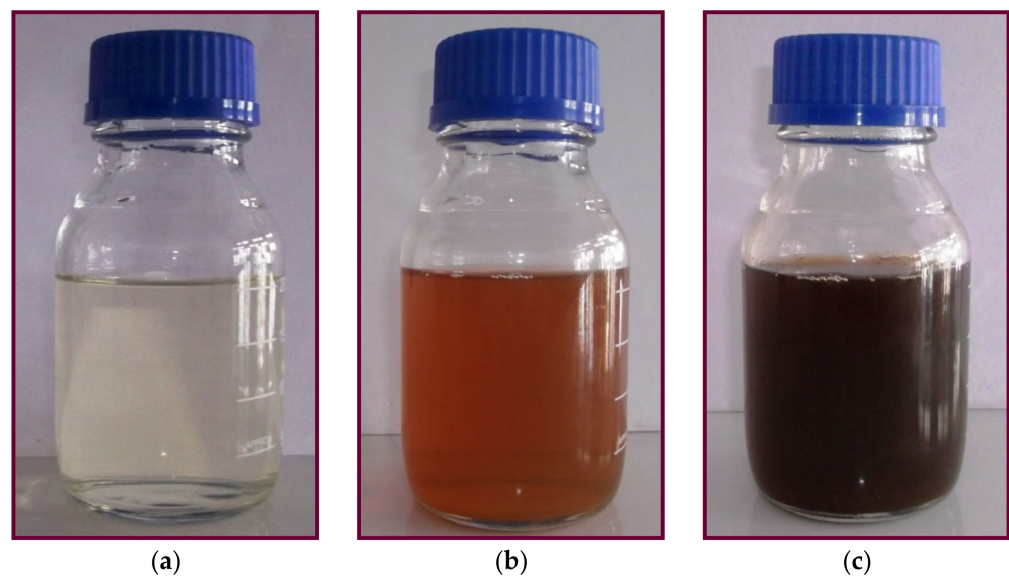
**Figure 1.** Change in color during the transition from a solution of silver nitrate to a suspension of silver nanoparticles; (**a**) near-colorless, 10 mM AgNO$_3$ solution with 10 mL of MCW extract; (**b**) brown, colloidal suspension of WS AgNPs obtained after successful nanonization; (**c**) intense cola-colored suspension of WS AgNPs obtained after optimization of nanonization conditions.

(**a**)



(**b**)
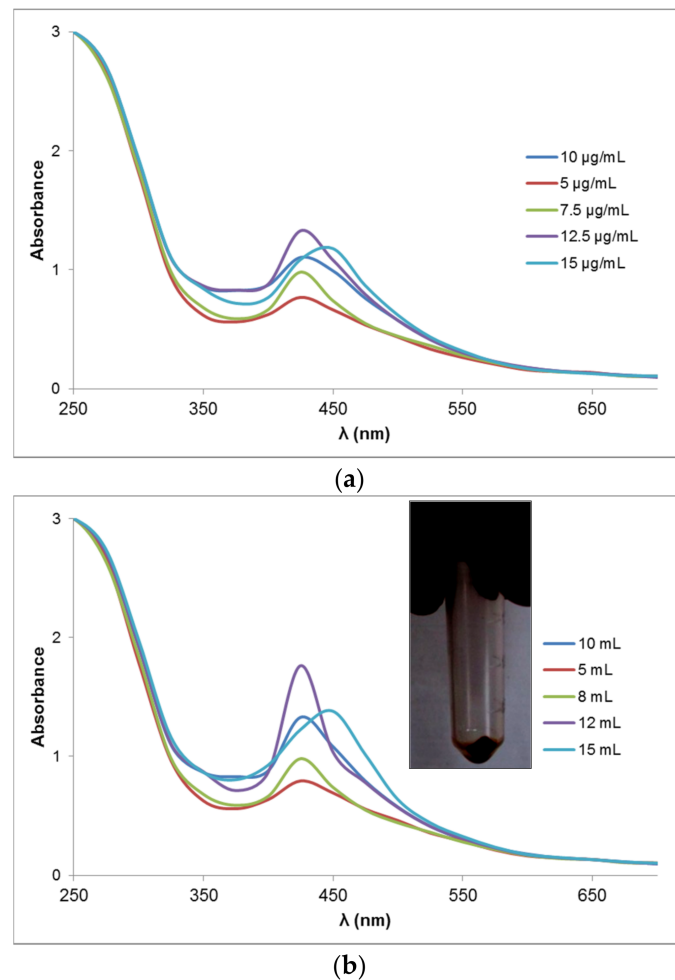
**Figure 2.** Optimization of reaction conditions for the yield of nanoparticles. (**a**) Effect of varying concentration of MCW extract on the formation of WS AgNPs: the dark blue curve (10 μg/mL) shows the UV-Vis absorption characteristics of the colloid of AgNPs obtained with the initial non-optimized reaction conditions; maximum yield of AgNPs was obtained when MCW extract was used at a concentration of 12.5 μg/mL. (**b**) Effect of varying volume of MCW extract on the formation of WS AgNPs: maximum AgNPs were obtained when 12 mL of MCW extract was used; the inset shows the AgNPs precipitated by centrifugation from 2 mL colloid when 12 mL of MCW extract (12.5 μg/mL) was used per 100 mL of 10 mM $AgNO_3$ for nanosynthesis.

FTIR spectroscopy was performed to confirm the inclusion of MCW extract in the nanoparticles. Figure 3a shows the FTIR transmittance of WS AgNPs. Spikes characteristic of the alcoholic group (hydrogen-bonded −OH stretch, 3625–3540 cm$^{-1}$), phenols (−OH stretch, 3625–3540 cm$^{-1}$; aromatic group C-C=C asymmetric stretch, ~1550–1450 cm$^{-1}$), coumarins (−OH stretch, 3625–3540 cm$^{-1}$; C=O group, 1080 cm$^{-1}$), terpenoids (−OH group, ~3400 cm$^{-1}$), flavonoids (C=O stretching, 1649 cm$^{-1}$), proteins (C-N group stretching and amide I band, 1382 cm$^{-1}$), and silver (broad peak, 1654 cm$^{-1}$) (Raut et al., 2014) were recorded. Figure 3b shows the X-ray diffraction pattern of the WS AgNPs; Bragg reflections with 2θ values corresponding to the 111, 200, and 220 sets of the lattice planes, respectively, were obtained. The average size of the green-synthesized WS AgNPs, assessed using the Debye–Scherrer equation [33] on the predominant Bragg reflection (2θ) 38.1, was determined as 9 nm. Similar findings were reported for the AgNPs obtained upon green synthesis with several plant extracts, including ginseng [34] and Indian ginseng [18,19].
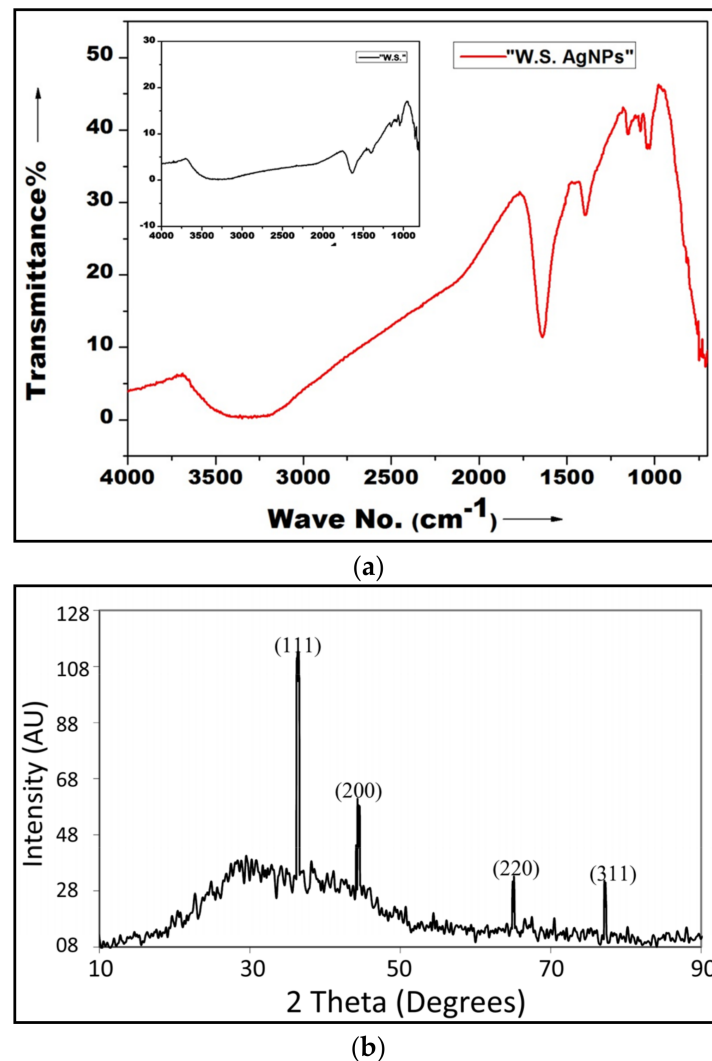
**Figure 3.** Characterization of WS AgNPs by FT-IR and XRD analyses. (**a**) FT-IR analysis shows the characteristic spikes of the alcoholic group (hydrogen-bonded –OH stretch, 3625–3540 cm$^{-1}$), phenols (–OH stretch, 3625–3540 cm$^{-1}$; aromatic group C-C=C asymmetric stretch, ~1550–1450 cm$^{-1}$), coumarins (–OH stretch, 3625–3540 cm$^{-1}$; C=O group, 1080 cm$^{-1}$), terpenoids (–OH group, ~3400 cm$^{-1}$), flavonoids (C=O stretching, 1649 cm$^{-1}$), alkanes (C-H group stretching, 1382 cm$^{-1}$), and silver (broad peak, 1654 cm$^{-1}$); the inset shows the FT-IR spectra of WS extract for comparison. (**b**) The X-ray diffraction pattern of AgNPs green-synthesized with extract of Indian ginseng shows diffraction peaks characteristic of 111, 200, 220, and 311 sets of lattice planes were observed in the 2 h range of 30–80, indicating the face-centered cubic (fcc) crystalline symmetry of the metallic silver in the nanoparticles.

Figure 4a shows the ultrastructure of the WS AgNPs from transmission electron microscopy of the nanoparticles; the uniformity of size and monodispersity of the AgNPs can be appreciated. The size–frequency of the WS AgNPs under TEM was plotted in a histogram (Figure 4b). Most (63%) of the WS AgNPs were in the 90–110 nm range. In total, 92% of the WS AgNPs were within the range of 80–120 nm, the mean size being 101.10 nm. Thus, the WS AgNPs were found to be of fairly uniform size. The apparent disparity in the size determination of AgNPs by XRD and TEM is common [18,19,33].

The results of the different assays performed for determining the cytotoxicity of WS AgNPs in CEF showed a good correlation. The non-cytotoxic doses of WS AgNPS determined by the AB, DPA, CV, MTT, and NR assays were 123.44 μg/mL, 69.30 μg/mL, 100.07 μg/mL, 105.99 μg/mL, and 113.60 μg/mL, respectively. The differences in the cytotoxicity of WS AgNPs determined by the assays were non-significant; however, the

differences in cytotoxicity of WS AgNPs at different concentrations were highly significant ($p < 0.01$). Based on a consensus of these assays, the maximum non-cytotoxic concentration of WS AgNPs for CEF was determined at 69.30 µg/mL. However, for the ease of dispensing and dilution, WS AgNPs were chosen to be used at a concentration of 65 µg/mL. The in vitro cytotoxicity of AgNPs is known to vary a lot depending on the particle size [8], method of synthesis [12], and cell type [35]. Seemingly contrary to previous studies, where AgNPs and silver ions were found not to induce DNA damage at non-cytotoxic doses [36], the DPA assay that measures cytotoxicity based on DNA content in the cells appeared to be most sensitive in our study. It is important to appreciate that the content of DNA need not necessarily correlate with the extent of DNA damage.
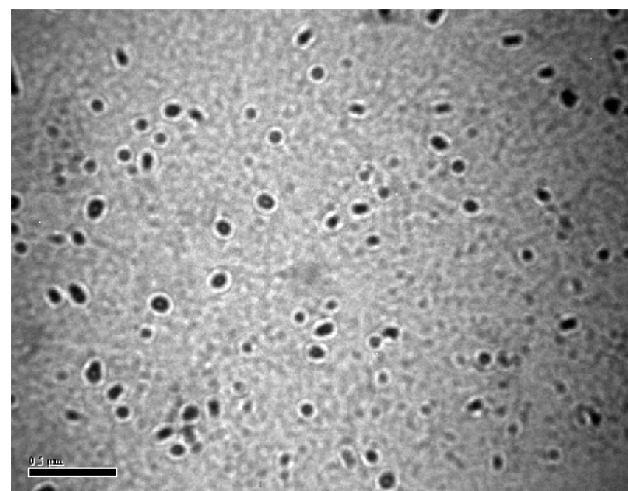


(**a**)
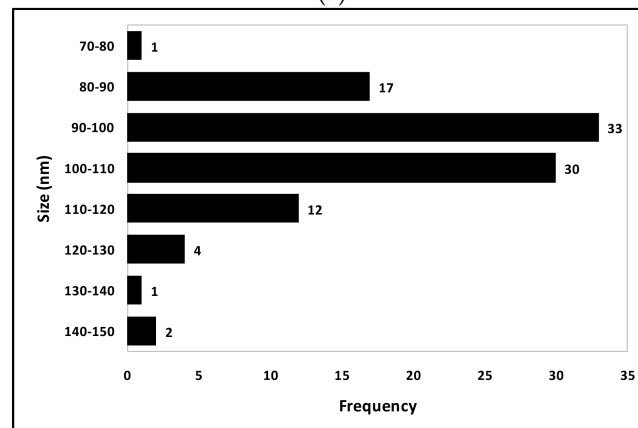


(**b**)

**Figure 4.** Transmission Electron Micrography of WS AgNPs. (**a**) Transmission electron micrograph of WS AgNPs. (**b**) The size distribution of WS AgNPs from TEM studies is shown; the mean diameter of the WS AgNPs based on the frequency distribution was 101.10 nm.

In the microtiter plate virus inhibition assay, the titer of the stock virus in CEF at 48 hpi was determined at $6.839 \times 10^4$ TCID$_{50}$/mL. CEF are a classical model for studying IBDV replication and cytopathy [37,38]. Kibenge et al. [29] reported titers varying from $2.238 \times 10^5$ TCID$_{50}$/ mL to $1.259 \times 10^6$ TCID$_{50}$/mL 25–30 hpi, albeit with a very different virus strain. In the presence of WS AgNPs, the titer at 48 hpi reduced significantly ($p < 0.01$) by nearly one order of magnitude to $4.704 \times 10^3$ TCID$_{50}$/mL, representing a decrease of approximately 93.12% (Figure 5a).

(a)



(b)



(c)
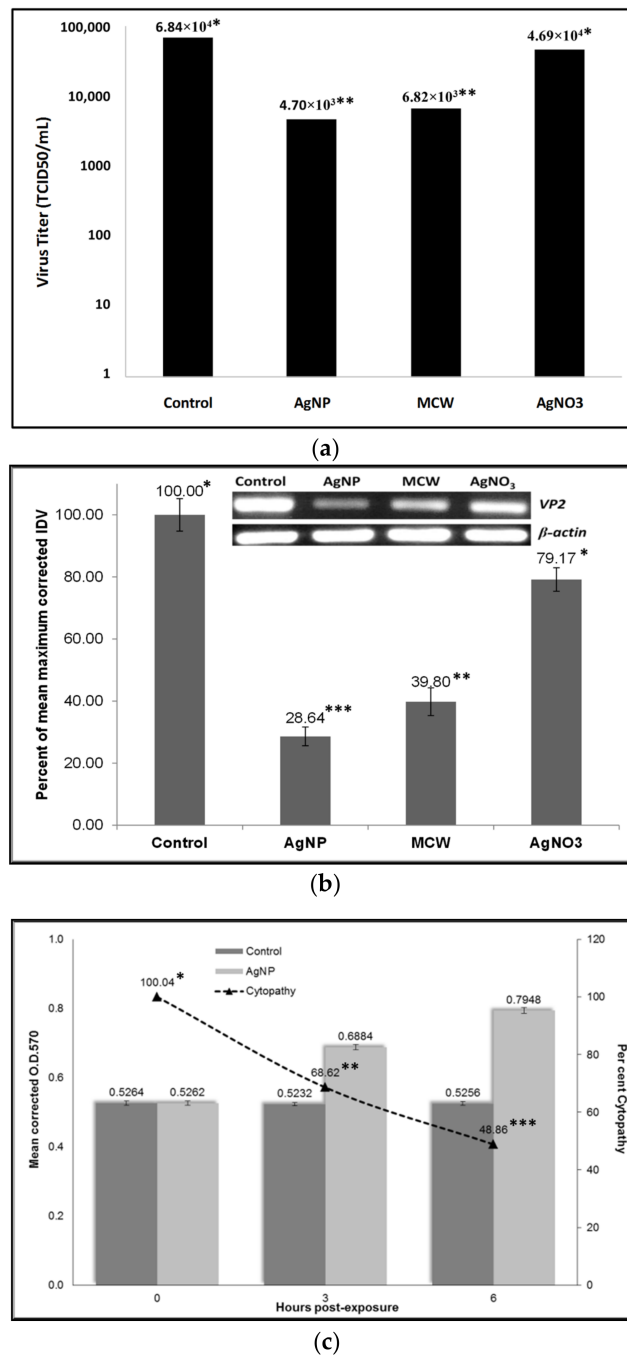
**Figure 5.** Results of virus inhibition assays. (**a**) Comparison of virus titer in IBDV-infected mock-treated control CEF and IBDV-infected CEF treated with WS AgNPs, MCW extract, or AgNO$_3$ solution; infected CEF were treated with 65 μg/mL WS AgNPs, 160 μg/mL MCW, or 5 mM AgNO$_3$ final concentration. (**b**) Relative semi-quantification of viral load in IBDV-infected mock-treated control CEF and IBDV-infected CEF treated with AgNPs, MCW extract, or AgNO$_3$ solution; integrated densitometric value (IDV) of RT-PCR product of *vp2* gene transcript segment was used for the relative semi-quantification of viral load whereas IDV of RT-PCR product of *β-actin* transcript (shown in inset) served as the control; infected CEF were treated with 65 μg/mL AgNP, 160 μg/mL MCW, or 5 mM AgNO$_3$ final concentration. (**c**) Effect of WS AgNP treatment on the ability of the virus to induce cytopathy in CEF; mock-treated virus or virus treated with WS AgNPs for 0, 3, or 6 h was allowed to infect CEF and cytopathy was determined at 48 hpi on the basis of MTT assay. All assays were performed in triplicate, and means were compared by ANOVA followed by Tukey's post hoc test. Values bearing a different number of asterisks differ significantly (*p* < 0.01) from each other.

Relative semi-quantification of the intracellular viral load was performed based on the integrated densitometric values (IDV) of the *vp2* gene using *β-actin* gene transcript as a control (Figure 5b). The differences between the groups were highly significant ($p < 0.01$), with AgNP-treated CEF revealing a 71.36% decrease in viral load compared to mock-treated CEF.

Co-incubation studies (Figure 5c) revealed that the virus co-incubated with WS AgNPs for 6 h exerted 51.14% lesser cytopathy as compared to the mock-treated virus. Moreover, the virus co-incubated with the WS AgNPs for a shorter duration induced significantly higher ($p < 0.01$) cytopathy than the virus co-incubated with WS AgNPs for a longer duration, possibly indicating a direct inhibitory effect of the WS AgNPs on the virion, which needs further validation. The few existing studies on the mechanism of virus inhibition by nanoparticles uphold this possibility since AgNPs have been shown to inhibit the virus by directly binding either to viral nucleic acids or to structural components such as glycoproteins [8,35,39].

IBDV is known to upset the apoptotic machinery of host cells, including CEF. During its replication in the bursal cells of chickens, cells infected by IBDV remain protected from undergoing apoptosis, whereas bystander cells undergo severe apoptotic changes [40]. AgNPs can have multiple cellular targets depending upon the cell type; AgNPs induce the mitochondrial apoptosis pathway in NIH3T3 fibroblast cells via ROS and JNK. AgNPs decrease intracellular glutathione, increase nitric oxide secretion, increase TNF-$\alpha$ transcript and protein levels, and increase the gene expression of matrix metalloproteinases (MMP), such as *MMP-3*, *MMP-11*, and *MMP-19* [41]. WS is also a well-known regulator of apoptosis; brought about by diverse mechanisms, it is capable of balancing pro- and anti-apoptotic mechanisms [25]. The synergistic activity of WS and nanosilver could be responsible for the anti-IBDV effect of WS AgNPs seen in the present study. All the previous reports on the virus-inhibitory effects of AgNPs were against enveloped RNA viruses, and the present study is novel because the IBD virus was non-enveloped. The presence of Indian ginseng extract, known to be inhibitory to IBDV [24–26], in the WS AgNPs may be responsible for this inhibitory activity. Some other viruses included in the family *Birnaviridae* are the infectious pancreatic necrosis virus, Tellina virus, oyster virus, yellow tail ascites virus and crab virus of the genus *Aquabirnavirus*, blotched snakehead virus of the genus *Blosnavirus*, and drosophila X virus of the genus *Entomobirnavirus* [42]; many of these are economically important pathogens. Birnaviruses also bear distinct evolutionary relationships to some other important viral pathogens, rotaviruses (*Reoviridae*) and picornaviruses (*Picornaviridae*), for example [43]. The results of the present study suggest that WS AgNPs may also inhibit such viruses. Nevertheless, all such mechanistic aspersions and extrapolative assumptions warrant further validation.

## 4. Conclusions

We studied the inhibitory effect of silver nanoparticles, green synthesized with an extract of *Withania somnifera* roots, against the infectious bursal disease virus of chickens using an in vitro chicken embryo fibroblast infection model. The optimum concentration and volume of root extract required for optimum nanosynthesis were determined by a two-step approach. The nanoparticles were characterized, and the non-cytotoxic dose of the nanoparticles for chicken embryo fibroblasts was determined. Co-incubation with the silver nanoparticles reduced the viral infectivity, decreased the intracellular viral load, and inhibited the cytopathy normally exerted by the virus. To the best of our knowledge, this is the first report on the inhibitory activity of green-synthesized silver nanoparticles against a non-enveloped virus. Our findings should encourage similar applications of the nanoparticles against other related veterinary and human viral pathogens.

**Author Contributions:** B.G. conceived and designed the study, synthesized and characterized the nanoparticles, performed toxicity and virus inhibition studies, analyzed the data, prepared the figures, and drafted the manuscript. A.K.V. participated in the characterizations of the plant material and the nanoparticles. B.S. performed electron microscopy. A.K.D., A.S. and I.G. secured funding for the

study and participated in the characterization of the nanoparticles. S.K.R., A.S. and I.G. participated in the conception and design of the study and revised the manuscript. D.L. participated in the validation. All authors have read and agreed to the published version of the manuscript.

**Conflicts of Interest:** The authors declare no conflict of interest.

**Dedication:** The authors dedicate this study to the fond memories of Balwinder Singh, who left the world on 5 June 2021 after braving a very long fight against COVID-19.

## References

1. Eterradossi, N.; Saif, Y.M. *Diseases of Poultry*, 14th ed.; Infectious Bursal Disease; John Wiley and Sons: Hoboken, NJ, USA, 2020; pp. 257–283. ISBN 9781119371199.
2. Van den Berg, T.P.; Eterradossi, N.; Toquin, D.; Meulemans, G. Infectious bursal disease (Gumboro disease). *Rev. Sci. Tech. Int. Off. Epizoot.* **2000**, *19*, 527–543.
3. Office International des Epizooties. Infectious bursal disease (Gumboro Disease). In *OIE International Animal Health Code: Mammals, Birds and Bees*, 8th ed.; OIE: Paris, France, 1995; pp. 247–248.
4. Dey, S.; Pathak, D.C.; Ramamurthy, N.; Maity, H.K.; Chellappa, M.M. Infectious bursal disease virus in chickens: Prevalence, impact, and management strategies. *Vet. Med. Res. Rep.* **2019**, *10*, 85–97. [CrossRef]
5. Ganguly, B.; Kumar, S.; Rastogi, S.K. Nanobiotechnologies for animal health and production. In *Biotechnology*; Ganguly, B., Dey, S., Govil, J.N., Eds.; Volume 1 (Animal Biotechnology); Studium Press: Houston, TX, USA, 2014; pp. 413–426.
6. Pangestika, R.; Ernawati, R. Antiviral activity effect of silver nanoparticles (AgNPs) solution against the growth of infectious bursal disease virus on embryonated chicken eggs with Elisa test. *KnE Life Sci.* **2017**, 536–548. [CrossRef]
7. Wai-YináSun, R.; SteveáLin, C.L. Silver nanoparticles fabricated in Hepes buffer exhibit cytoprotective activities toward HIV-1 infected cells. *Chem. Commun.* **2005**, *40*, 5059–5061.
8. Lu, L.; Sun, R.W.; Chen, R.; Hui, C.K.; Ho, C.M.; Luk, J.M.; Lau, G.K.; Che, C.M. Silver nanoparticles inhibit hepatitis B virus replication. *Antivir. Ther.* **2008**, *13*, 253–262. [CrossRef]
9. Rogers, J.V.; Parkinson, C.V.; Choi, Y.W.; Speshock, J.L.; Hussain, S.M. A Preliminary Assessment of Silver Nanoparticle Inhibition of Monkeypox Virus Plaque Formation. *Nanoscale Res. Lett.* **2008**, *3*, 129–133. [CrossRef]
10. Baram-Pinto, D.; Shukla, S.; Perkas, N.; Gedanken, A.; Sarid, R. Inhibition of Herpes Simplex Virus Type 1 Infection by Silver Nanoparticles Capped with Mercaptoethane Sulfonate. *Bioconjug. Chem.* **2009**, *20*, 1497–1502. [CrossRef]
11. Chen, N.; Zheng, Y.; Yin, J.; Li, X.; Zheng, C. Inhibitory effects of silver nanoparticles against adenovirus type 3 in vitro. *J. Virol. Methods* **2013**, *193*, 470–477. [CrossRef]
12. Gaikwad, S.; Ingle, A.; Gade, A.; Rai, M.; Falanga, A.; Incoronato, N.; Russo, L.; Galdiero, S.; Galdiero, M. Antiviral activity of mycosynthesized silver nanoparticles against herpes simplex virus and human parainfluenza virus type 3. *Int. J. Nanomed.* **2013**, *8*, 4303–4314. [CrossRef]
13. Mori, Y.; Ono, T.; Miyahira, Y.; Nguyen, V.Q.; Matsui, T.; Ishihara, M. Antiviral activity of silver nanoparticle/chitosan composites against H1N1 influenza A virus. *Nanoscale Res. Lett.* **2013**, *8*, 93. [CrossRef]
14. Trefry, J.C.; Wooley, D.P. Silver nanoparticles inhibit vaccinia virus infection by preventing viral entry through a macropinocytosis-dependent mechanism. *J. Biomed. Nanotechnol.* **2013**, *9*, 1624–1635. [CrossRef] [PubMed]
15. Xiang, D.; Zheng, Y.; Duan, W.; Li, X.; Yin, J.; Shigdar, S.; O'Connor, M.L.; Marappan, M.; Zhao, X.; Miao, Y.; et al. Inhibition of A/Human/Hubei/3/2005 (H3N2) influenza virus infection by silver nanoparticles in vitro and in vivo. *Int. J. Nanomed.* **2013**, *8*, 4103–4113. [CrossRef] [PubMed]
16. Khandelwal, N.; Kaur, G.; Chaubey, K.K.; Singh, P.; Sharma, S.; Tiwari, A.; Singh, S.V.; Kumar, N. Silver nanoparticles impair Peste des petitsruminants virus replication. *Virus Res.* **2014**, *190*, 1–7. [CrossRef]
17. Sharma, V.; Kaushik, S.; Pandit, P.; Dhull, D.; Yadav, J.P.; Kaushik, S. Green synthesis of silver nanoparticles from medicinal plants and evaluation of their antiviral potential against chikungunya virus. *Appl. Microbiol. Biotechnol.* **2019**, *103*, 881–891. [CrossRef]
18. Raut, R.W.; Mendhulkar, V.D.; Kashid, S.B. Photosensitized synthesis of silver nanoparticles using Withania somnifera leaf powder and silver nitrate. *J. Photochem. Photobiol. B Biol.* **2014**, *132*, 45–55. [CrossRef] [PubMed]
19. Marslin, G.; Selvakesavan, R.K.; Franklin, G.; Sarmento, B.; Dias, A.C. Antimicrobial activity of cream incorporated with silver nanoparticles biosynthesized from Withania somnifera. *Int. J. Nanomed.* **2015**, *10*, 5955. [CrossRef]

20. Singh, S.; Kumar, S. *Withania somnifera: The Indian Ginseng Ashwagandha*; Central Institute of Medicinal and Aromatic Plants: Lucknow, India, 1998.

21. Hepper, F.N. Old world Withania (Solanaceae): A taxonomic review and key to the species. In *Solanaceae III: Txonomy, Chemitry, Evolution*; Royal Botanic Gardens, Kew: London, UK, 1991; pp. 211–227.

22. Singh, P.; Sharma, Y.K. Withania somnifera (ashwagandha): A wonder herb with multiple medicinal properties. *Asian J. Pharm. Pharmacol.* **2018**, *4*, 123–130. [CrossRef]

23. Ganguly, B.; Kumar, N.; Ahmad, A.H.; Rastogi, S.K. Influence of phytochemical composition on in vitro antioxidant and reducing activities of Indian ginseng [*Withania somnifera* (L.) Dunal] root extracts. *J. Ginseng Res.* **2018**, *42*, 463–469. [CrossRef]

24. Ganguly, B.; Kumar, S.; Umapathi, V.; Ambwani, T. Inhibition of Gumboro virus by *Withania somnifera* extract. In Proceedings of the 5th Uttarakhand State Science and Technology Congress, Uttarakhand Council for Science and Technology, Abstracts and Souvenir, Doon University, Dehradun, India, 10–12 November 2010; p. 315.

25. Ganguly, B.; Umapathi, V.; Rastogi, S.K. Nitric oxide induced by Indian ginseng root extract inhibits Infectious Bursal Disease virus in chicken embryo fibroblasts in vitro. *J. Anim. Sci. Technol.* **2018**, *60*, 2. [CrossRef]

26. Ganguly, B.; Mrigesh, M.; Chauhan, P.; Rastogi, S.K. Dietary supplementation with Withania somnifera root powder ameliorates experimentally induced Infectious Bursal Disease in chicken. *Trop. Anim. Health Prod.* **2020**, *52*, 1195–1206. [CrossRef]

27. Chang, C.Y.; Walther, P.J.; McDonnell, D.P. Glucocorticoids manifest androgenic activity in a cell line derived from a metastatic prostate cancer. *Cancer Res.* **2001**, *61*, 8712–8717. [PubMed]

28. Pretorius, E.; Oberholzer, H.; Becker, P. Comparing the cytotoxic potential of *Withania somnifera* water and methanol extracts. *Afr. J. Tradit. Complement. Altern. Med.* **2009**, *6*, 275–280. [CrossRef]

29. Kibenge, F.S.; Dhillon, A.S.; Russell, R.G. Biochemistry and immunology of Infectious Bursal Disease virus. *J. Gen. Virol.* **1988**, *69*, 1757–1775. [CrossRef]

30. Hamilton, M.A.; Russo, R.C.; Thurston, R.V. Trimmed Spearman-Karber method for estimating median lethal concentrations in toxicity bioassays. *Environ. Sci. Technol.* **1977**, *7*, 714–719. [CrossRef]

31. Ahmad, A.; Mukherjee, P.; Senapati, S.; Mandal, D.; Khan, M.I.; Kumar, R.; Sastry, M. Extracellular biosynthesis of silver nanoparticles using the fungus Fusarium oxysporum. *Colloids Surf. B Biointerfaces* **2003**, *28*, 313–318. [CrossRef]

32. Giannenas, I.; Sidiropoulou, E.; Bonos, E.; Christaki, E.; Floro -Paneri, P. The history of herbs, medicinal and aromatic plants, andtheir extracts: Past, current situation and future perspectives. In *Feed Additives: Aromatic Plants and Herbs in Animal Nutrition and Health*; Florou-Paneri, P., Christaki, E., Giannenas, I., Eds.; Elsevier: London, UK, 2019; pp. 1–18. ISBN 978-0-12-814700-9.

33. Anandalakshmi, K.; Venugobal, J.; Ramasamy, V. Characterization of silver nanoparticles by green synthesis method using Pedalium murex leaf extract and their antibacterial activity. *Appl. Nanosci.* **2016**, *6*, 399–408. [CrossRef]

34. Sreekanth, T.V.M.; Nagajyothi, P.C.; Muthuraman, P.; Enkhtaivan, G.; Vattikuti, S.V.P.; Tettey, C.O.; Kim, D.H.; Shim, J.; Yoo, K. Ultra-sonication-assisted silver nanoparticles using Panax ginseng root extract and their anti-cancer and antiviral activities. *J. Photochem. Photobiol. B Biol.* **2018**, *188*, 6–11. [CrossRef]

35. Lara, H.H.; Ayala-Nunez, N.V.; Ixtepan-Turrent, L.; Rodriguez-Padilla, C. Mode of antiviral action of silver nanoparticles against HIV-1. *J. Nanobiotechnol.* **2010**, *8*, 1. [CrossRef]

36. Zhang, X.F.; Shen, W.; Gurunathan, S. Silver nanoparticle-mediated cellular responses in various cell lines: An in vitro model. *Int. J. Mol. Sci.* **2016**, *17*, 1603. [CrossRef]

37. Lukert, P.D.; Davis, R.B. Infectious Bursal Disease virus: Growth and characterization in cell cultures. *Avian Dis.* **1974**, *18*, 243–250. [CrossRef]

38. McNulty, M.S.; Allan, G.M.; McFerran, J.B. Isolation of Infectious Bursal Disease virus from turkeys. *Avian Pathol.* **1979**, *8*, 205–212. [CrossRef] [PubMed]

39. Elechiguerra, J.L.; Burt, J.L.; Morones, J.R.; Camacho-Bragado, A.; Gao, X.; Lara, H.H.; Yacaman, M.J. Interaction of silver nanoparticles with HIV-1. *J. Nanobiotechnol.* **2005**, *3*, 6. [CrossRef] [PubMed]

40. Jungmann, A.; Nieper, H.; Muller, H. Apoptosis is induced by infectious bursal disease virus replication in productively infected cells as well as in antigen negative cells in their vicinity. *J. Gen. Virol.* **2001**, *82*, 1107–1115. [CrossRef] [PubMed]

41. Lara, H.H.; Garza-Treviño, E.N.; Ixtepan-Turrent, L.; Singh, D.K. Silver nanoparticles are broad-spectrum bactericidal and virucidal compounds. *J. Nanobiotechnol.* **2011**, *9*, 30. [CrossRef]

42. ICTV (International Committee on Taxonomy of Viruses) 2011. Virus Taxonomy. 2011. Available online: http://www.ictvonline.org/virusTaxonomy.asp (accessed on 28 February 2015).

43. Dalton, R.M.; Rodríguez, J.F. Rescue of Infectious Birnavirus from Recombinant Ribonucleoprotein Complexes. *PLoS ONE* **2014**, *9*, e87790. [CrossRef]